

NUCLEAR DATA AND MEASUREMENTS SERIES

ANL/NDM-125

**Fast-Neutron Scattering
Near Shell Closures: Scandium**

by

A.B. Smith and P.T. Guenther

August 1992

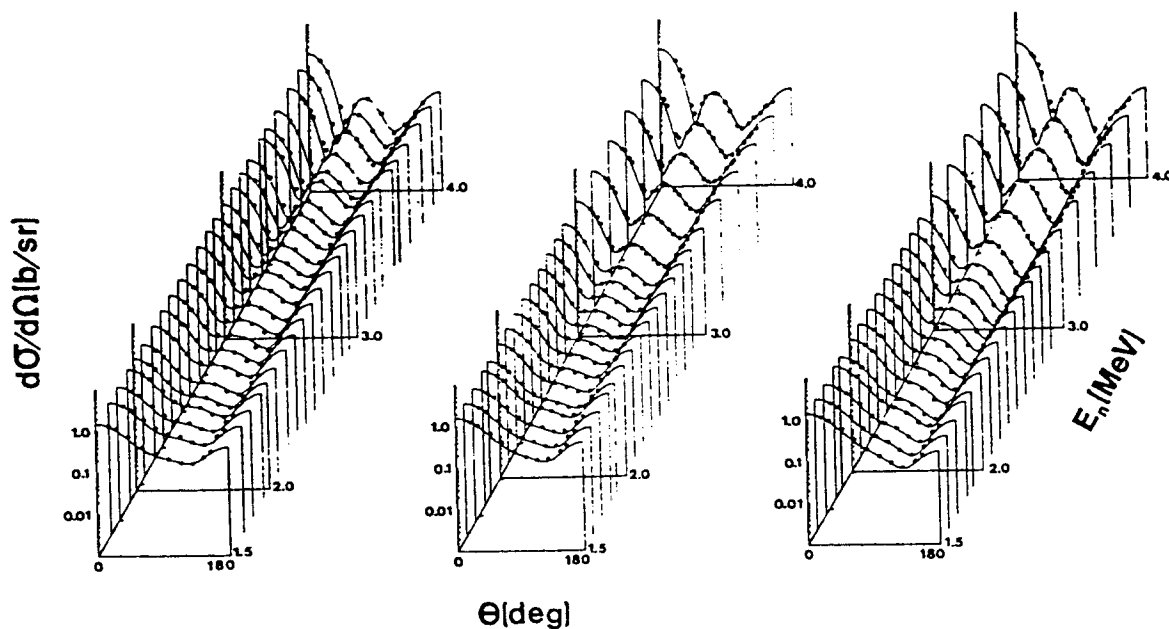
**ARGONNE NATIONAL LABORATORY,
ARGONNE, ILLINOIS 60439, U.S.A.**

NUCLEAR DATA AND MEASUREMENTS SERIES

ANL/NDM-125

FAST-NEUTRON SCATTERING NEAR SHELL CLOSURES:-
SCANDIUM

A. B. Smith and P. T. Guenther
August 1992



ARGONNE NATIONAL LABORATORY, ARGONNE, ILLINOIS

Operated by THE UNIVERSITY OF CHICAGO

for the U. S. DEPARTMENT OF ENERGY

under Contract W-31-109-Eng-38

Argonne National Laboratory, with facilities in the states of Illinois and Idaho, is owned by the United States government, and operated by The University of Chicago under the provisions of a contract with the Department of Energy.

DISCLAIMER

This report was prepared as an account of work sponsored by an agency of the United States Government. Neither the United States Government nor any agency thereof, nor any of their employees, makes any warranty, express or implied, or assumes any legal liability or responsibility for the accuracy, completeness, or usefulness of any information, apparatus, product, or process disclosed, or represents that its use would not infringe privately owned rights. Reference herein to any specific commercial product, process, or service by trade name, trademark, manufacturer, or otherwise, does not necessarily constitute or imply its endorsement, recommendation, or favoring by the United States Government or any agency thereof. The views and opinions of authors expressed herein do not necessarily state or reflect those of the United States Government or any agency thereof.

Reproduced from the best available copy.

Available to DOE and DOE contractors from the
Office of Scientific and Technical Information
P.O. Box 62

Oak Ridge, TN 37831

Prices available from (615) 576-8401

Available to the public from the
National Technical Information Service
U.S. Department of Commerce

5285 Port Royal Road
Springfield, VA 22161

ANL/NDM-125

FAST-NEUTRON SCATTERING NEAR SHELL CLOSURES:- SCANDIUM*

by

A. B. Smith and P. T. Guenther

Keywords:

Measured $d\sigma/d\Omega_{el}$ and $d\sigma/d\Omega_{inel}$ for 1.5 - 10.0 MeV neutrons incident on scandium. Physical interpretation. Optical-statistical and Dispersive-optical models.

Engineering Physics Division
Argonne National Laboratory
9700 South Cass Avenue
Argonne, Illinois 60439
U. S. A

* This work supported by the United States Department of Energy under Contract W-31-109-Eng-38.

NOTICE

For approximately a third of a century, the Applied Nuclear Physics Section, Engineering Physics Division, Argonne National Laboratory, has been a primary world source of neutron and nuclear data requiring monenergetic neutron-source capabilities (e.g., neutron activation, neutron scattering, etc. data). It is with regret that I must inform you that the United States Department of Energy has ordered that the relevant Fast Neutron Generator Facility be shut down. The associated expertise developed over these many years will vanish. There remains a wealth of unique data to be analyzed and presented. To the extent possible, this work will be completed over the coming months. This document is the first such concluding report. Some of the authors can be contacted at the Argonne National Laboratory should more information be desired.

Over the years it has been my privileged and pleasure to know many of you across the world. To each of you my very best personal and professional wishes.

Alan Bowen Smith

Argonne, July 1992.

TABLE OF CONTENTS

| | |
|--|----|
| Prior Issues in this Report Series ----- | v |
| Abstract ----- | ix |
| I. Introduction ----- | 1 |
| II. Experimental Methods ----- | 1 |
| III. Measured Results ----- | 2 |
| IV. Physical Models | |
| A. Optical-Statistical Model ----- | 7 |
| B. Dispersive Optical Model----- | 15 |
| V. Discussion ----- | 17 |
| References ----- | 26 |

PRIOR ISSUES IN THE ANL/NDM SERIES

A listing of recent issues in this series is given below. Issues and/or titles prior to ANL/NDM-100 can be obtained from the National Technical Information Service, U. S. Department of Commerce, 5285 Port Royal Road, Springfield, VA 22161, or by contacting one of the authors of this report at the following address:-

Engineering Physics Division
Argonne National Laboratory
9700 South Cass Avenue
Argonne, IL 60439
USA

- A.B. SMITH, P.T. GUENTHER AND R.D. LAWSON
The Energy Dependence of the Optical-Model Potential for Fast-Neutron Scattering From Bismuth
ANL/NDM-100 (1987)
- A.B. SMITH, P.T. GUENTHER, J.F. WHALEN AND R.D. LAWSON
Cobalt, Fast Neutrons and Physical Models
ANL/NDM-101 (1987)
- D.L. SMITH
Investigation of the Influence of the Neutron Spectrum in Determinations of Integral Neutron Cross-Section Ratios
ANL/NDM-102 (1987)
- A.B. SMITH, P. GUENTHER and B. MICKLICH
Spectrum of Neutrons Emitted From a Thick Beryllium Target Bombarded With 7 MeV Deuterons
ANL/NDM-103 (1988)
- L.P. GERALDO and D.L. SMITH
Some Thoughts on Positive Definiteness in the Consideration of Nuclear Data Covariance Matrices
ANL/NDM-104 (1988)
- A. B. SMITH, D.L. SMITH, P.T. GUENTHER, J.V. MEADOWS, R. D. LAWSON, R.J. HOWERTON, and T. DJEMIL
Neutronic Evaluated Nuclear Data File for Vanadium
ANL/NDM-105 (1988)
- A.B. SMITH, P.T. GUENTHER, AND R.D. LAWSON
Fast-Neutron Elastic Scattering from Elemental Vanadium
ANL/NDM-106 (1988)
- P.T. GUENTHER, R.D. LAWSON, M. SUGIMOTO, A.B. SMITH, AND D.L. SMITH
An Evaluated Neutronic Data File for Elemental Cobalt
ANL/NDM-107 (1988)

- M. SUGIMOTO, P.T. GUENTHER, J.E. LYNN, A.B. SMITH, AND J.F. WHALEN
Some Comments on the Interaction of Fast-Neutrons with Beryllium
 ANL/NDM-108 (1988)
- P.T. GUENTHER, R.D. LAWSON, J.V. MEADOWS, A.B. SMITH, D.L. SMITH, AND
 M. SUGIMOTO
An Evaluated Neutronic Data File for Bismuth
 ANL/NDM-109 (March 1989)
- D.L. SMITH AND L.P. GERALDO
A Vector Model for Error Propagation
 ANL/NDM-110 (March 1989)
- J.E. LYNN
Fifty Years of Nuclear Fission
 ANL/NDM-111 (June 1989)
- S. CHIBA, P.T. GUENTHER, AND A.B. SMITH
*Some Remarks on the Neutron Elastic- and Inelastic-Scattering
 Cross Sections of Palladium*
 ANL/NDM-112 (May 1989)
- J.E. LYNN
Resonance Effects in Neutron Scattering Lengths
 ANL/NDM-113 (June 1989)
- A.B. SMITH, R.D. LAWSON, AND P.T. GUENTHER
*Ambiguities in the Elastic Scattering of 8 MeV neutrons from
 Adjacent Nuclei*
 ANL/NDM-114, January 1990
- A.B. SMITH, S. CHIBA, D.L. SMITH, J.V. MEADOWS, P.T. GUENTHER, R.D.
 LAWSON, AND R.J. HOVERTON
Evaluated Neutronic File for Indium
 ANL/NDM-115, January 1990
- S. CHIBA, P.T. GUENTHER, R.D. LAWSON, AND A.B. SMITH
*Neutron Scattering from Elemental Indium, the Optical Model, and
 the Bound-State Potential*
 ANL/NDM-116, June 1990
- D.L. SMITH AND L.P. GERALDO
*An Evaluation of the Nb-93(n,n')Nb-93m Dosimeter Reaction for
 ENDF/B-VI*
 ANL/NDM-117 (November 1990)
- J.V. MEADOWS
*Characteristics of the Samples in the FNG Fission Deposit
 Collection*
 ANL/NDM-118 (November 1990)

- S. CHIBA, P. T. GUENTHER, A. B. SMITH, M. SUGIMOTO, AND R. D. LAVSON
Fast-Neutron Interaction with Elemental Zirconium, and the Dispersive Optical Model
ANL/NDM-119, June 1991
- A. B. SMITH, P. T. GUENTHER, J. F. WHALEN, AND S. CHIBA
Fast-neutron Total and Scattering Cross Sections of ^{58}Ni and Nuclear Models
ANL/NDM-120, July 1991
- S. CHIBA AND D. L. SMITH
A Suggested Procedure for Resolving an Anomaly in Least-squares Data Analysis Known as "Peelle's Pertinent Puzzle" and the General Implications for Nuclear Data Evaluation
ANL/NDM-121, September 1991
- D. L. SMITH AND DOMINIQUE FEAUTRIER
Development and Testing of a Deuterium Gas Target Assembly for Neutron Production Via the $\text{H-2}(D,N)\text{H-3}$ Reaction at a Low-energy Accelerator Facility
ANL/NDM-122, March 1992
- D. L. SMITH AND E. T. CHENG
A Review of Nuclear Data Needs and Their Status for Fusion Reactor Technology with some Suggestions on a Strategy to Satisfy the Requirements
ANL/NDM-123, September 1991
- J. W. MEADOWS
The Thick-Target $^9\text{Be}(d,n)$ Neutron Spectra for Deuteron Energies Between 2.6 and 7.0-MeV
ANL/NDM-124, November 1991

ANL/NDM-125

FAST NEUTRON SCATTERING NEAR SHELL CLOSURES:- SCANDIUM

by

A. B. Smith and P. T. Guenther
Argonne National Laboratory
Argonne, Illinois

ABSTRACT

Neutron differential elastic- and inelastic-scattering cross sections are measured from from ≈ 1.5 to 10 MeV with sufficient detail to define the energy-averaged behavior of the scattering processes. Neutrons corresponding to excitations of 465 ± 23 , 737 ± 20 , 1017 ± 34 , 1251 ± 20 , 1432 ± 23 and 1692 ± 25 keV are observed. It is shown that the observables, including the absorption cross section, are reasonably described with a conventional optical-statistical model having energy-dependent geometric parameters. These energy dependencies are alleviated when the model is extended to include the contributions of the dispersion relationship. The model parameters are conventional, with no indication of anomalous behavior of the neutron interaction with ^{45}Sc , five nucleons from the doubly closed shell at ^{40}Ca .

I. INTRODUCTION

Problems have repeatedly been experienced in attempting to physically interpret fast-neutron scattering from the doubly closed-shell nucleus ^{40}Ca [1,2] at lower energies where compound-nucleus contributions to the scattering processes are significant. The issue remains unresolved, and is under continued investigation. In an attempt to cast some light on this question, the present experimental study, and associated physical interpretations, of fast-neutron scattering from the next higher naturally-available isotone, ^{45}Sc , was undertaken. The element is mono-isotopic, and is readily available in high-purity form. However, it is an odd-spin target with a $0f_{7/2}$ ground state and a very low-lying (12.4 keV) $0d_{3/2}^{-1}$ first-excited state. Inelastic-neutron scattering resulting in the excitation of the latter low-lying level is not experimentally resolved from the elastically-scattered component. As a consequence, analytical artifices must be used in the physical interpretation at some compromise in accuracy.

The national evaluated file system, ENDF/B-VI, contains limited dosimetry information for scandium; there is no general purpose neutronic file. With the measurements of this work and the associated physical interpretations, a comprehensive evaluated neutronic data file was obtained, as discussed in the companion document of ref. [3]

Subsequent portions of this report address:- i) a brief outline of the measurement methods, ii) the experimental results, iii) the physical interpretation in the context of both spherical and dispersive optical-statistical models, and iv) finally, some summary comments.

II. EXPERIMENTAL METHODS

All of the measurements of this work were made using the time-of-flight technique and the Argonne 10-angle scattering apparatus [4]. The application of these techniques at Argonne National Laboratory has been extensively described elsewhere [5-7], therefore only brief remarks relevant to these particular measurements are made here. In this particularly study, where detailed information must be obtained in a fluctuating cross-section environment, the efficiency and stability achievable with the 10-angle detection system is a valued attribute.

A single cylindrical sample of elemental scandium, 2 cm in

diameter and 2 cm in height, was employed in all of the measurements. The chemical purity was > 99%, and similar-sized samples of pile-grade graphite and polyethylene were employed for normalization purposes. The sample density was determined by weight and dimensional measurements to a precision of better than 0.5%.

At incident neutron energies of ≤ 4 MeV the ${}^7\text{Li}(p,n){}^7\text{Be}$ reaction was used as a neutron source [8]. The lithium was in the form of a thin metal film, with the thickness adjusted to give the desired incident-energy resolution. At incident neutron energies of > 4 MeV the $\text{D}(d,n){}^3\text{He}$ reaction was used as the neutron source [8]. The deuterium was contained in a gas cell with the pressures adjusted to obtain the desired incident-neutron energy resolution. Both sources were pulsed at a repetition rate of 2 MHz with a burst duration of ≈ 1 ns. Intensities were enhanced through the use of a harmonic bunching system. The scattering sample was placed approximately 18 cm from the source at a 0° source-reaction angle. The scattered-neutron spectra were measured by timing the transit of the scattered neutrons over flight paths of ≈ 5 m. The scattered-neutron detectors were liquid scintillators ≈ 12.5 cm in diameter, and either ≈ 2.5 or 6 cm thick, depending upon the incident-neutron energy, with the thicker detectors being used above incident-neutron energies of ≈ 4 MeV. The relative efficiencies of these detectors were determined using the ${}^{252}\text{Cf}$ fission spectrum, as described in ref. [9]. The angular scale of the measurement system was determined to $\approx 0.1^\circ$ by observation of neutrons elastically-scattered from a heavy target (e.g., niobium) on either side of the center line at forward angles where the elastic scattering is very rapidly varying with angle. Scattered-neutron energy resolutions were ≈ 0.5 ns/m. At incident energies of ≤ 4 MeV, the cross sections were determined relative to the well known total cross sections of elemental carbon in the manner described in ref. [10]. Above 4 MeV the cross sections were determined relative to the $\text{H}(n,n)$ standard cross section [11]. All of the experimental results were corrected for multiple-event, beam-attenuation and angular-resolution effects using the Monte-Carlo methods of ref. [12]. These methods included corrections for the second neutron group emitted from the ${}^7\text{Li}(p,n){}^7\text{Be}^*$ source reaction. The latter were important in the context of inelastically-scattered neutrons.

III. MEASURED RESULTS

A. Elastic Neutron Scattering

The scattering measurements were made from ≈ 1.5 to 4 MeV, at ten angles distributed between $\approx 25^\circ$ and 150° . The primary experimental

concern was the determination of the energy-average behavior of a cross section that undoubtedly is rapidly fluctuating with energy. Therefore the measurements at energies of ≤ 3 MeV were made at ≈ 50 keV incident-energy intervals with incident-energy spreads of ≈ 50 keV so that, on the average, the entire energy interval was sampled. In order to further smooth the cross section fluctuations, a running 150 keV average of the measured elastic-scattering results was constructed. Of course, the relatively broad incident-energy spreads required for the averaging compromised the scattered-neutron resolutions associated with the observation of the inelastically-scattered neutron groups. Moreover, in no observation were the neutrons due to the inelastic excitation of the 12.4 keV ($3/2^+$) level resolved from the elastically-scattered contribution. From 3 to 4 MeV it was assumed that the effect of fluctuations is considerably reduced, therefore the incident-energy measurement interval was extended from 50 to 100 keV. The individual differential cross section values were believed known to $\leq 5\%$, including statistical and systematic contributions associated with both the sample and normalization aspects of the measurements. The measured results below 4 MeV are summarized in Fig. III-1.

Above incident-neutron energies of 4 MeV, the elastic-scattering measurements were made at incident-neutron energy intervals of ≈ 0.5 MeV, with 30 to 60 differential values for each distribution spanning an angular range of $\approx 20^\circ$ to 160° . Incident neutron energy spreads varied from ≈ 300 keV at 4.5 MeV to ≈ 100 keV at 10 MeV. The uncertainties associated with the individual differential values varied from $\approx 3\%$ in regions of prominent cross sections to larger values in the minima of the distributions, inclusive of both systematic and statistical contributions. The experimental elastic-scattering results above 4 MeV, together with broad energy averages of the lower energy results, are shown in Fig. III-2.

Apparently, no scandium elastic scattering distributions have been reported in the literature comparable with the results of the present work. Barnard et al. [13] have made a very detailed study at incident energies below ≈ 1.4 MeV. Their results show large resonance fluctuations, but on the energy average they reasonably extrapolate to the lower-energy limit of the present work.

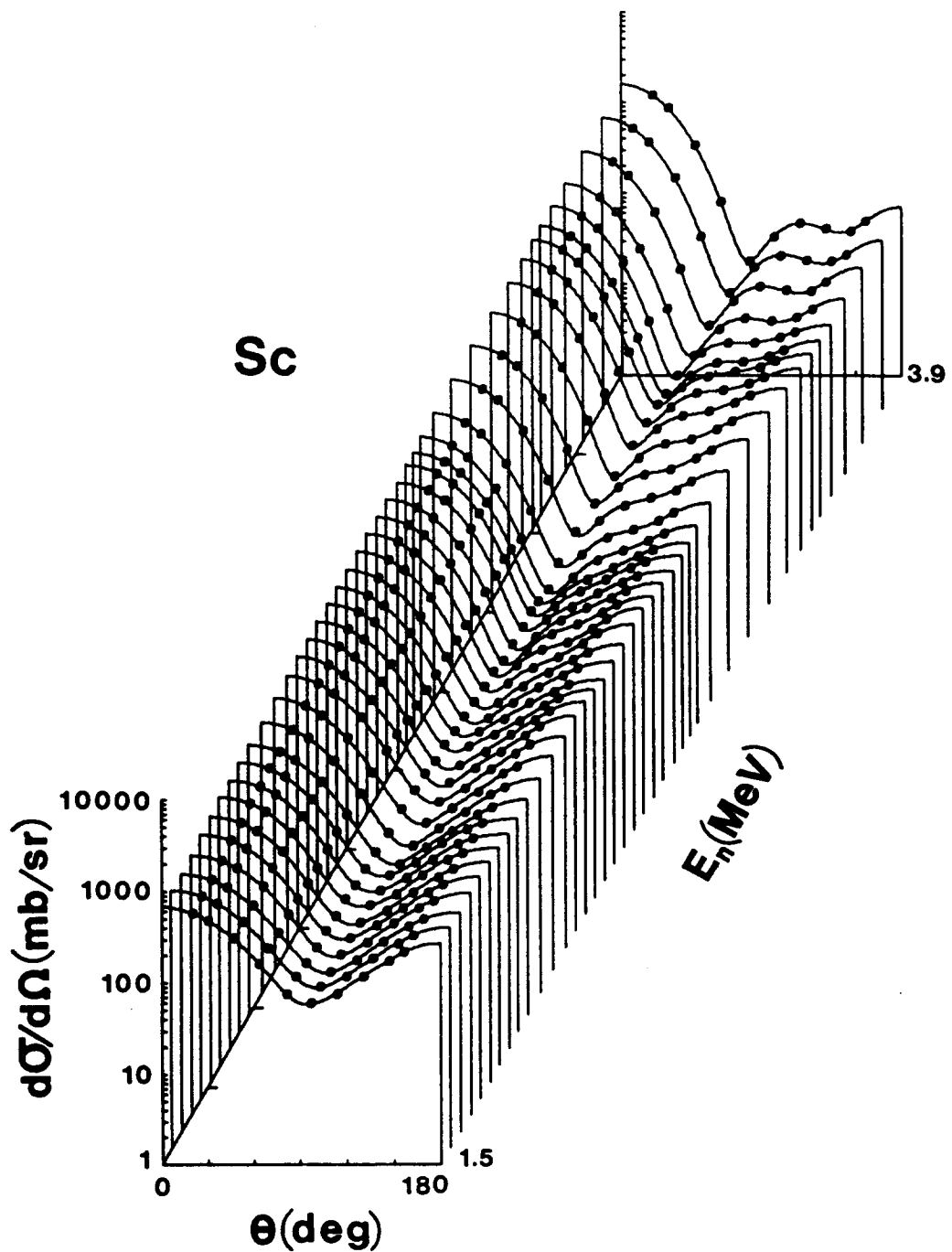


Fig. III-1. Measured differential elastic-scattering cross sections of scandium (symbols). Curves indicate the results of fitting the measured values with a Legendre-polynomial expansion. Here, and throughout this paper, results are given in the laboratory coordinate system.

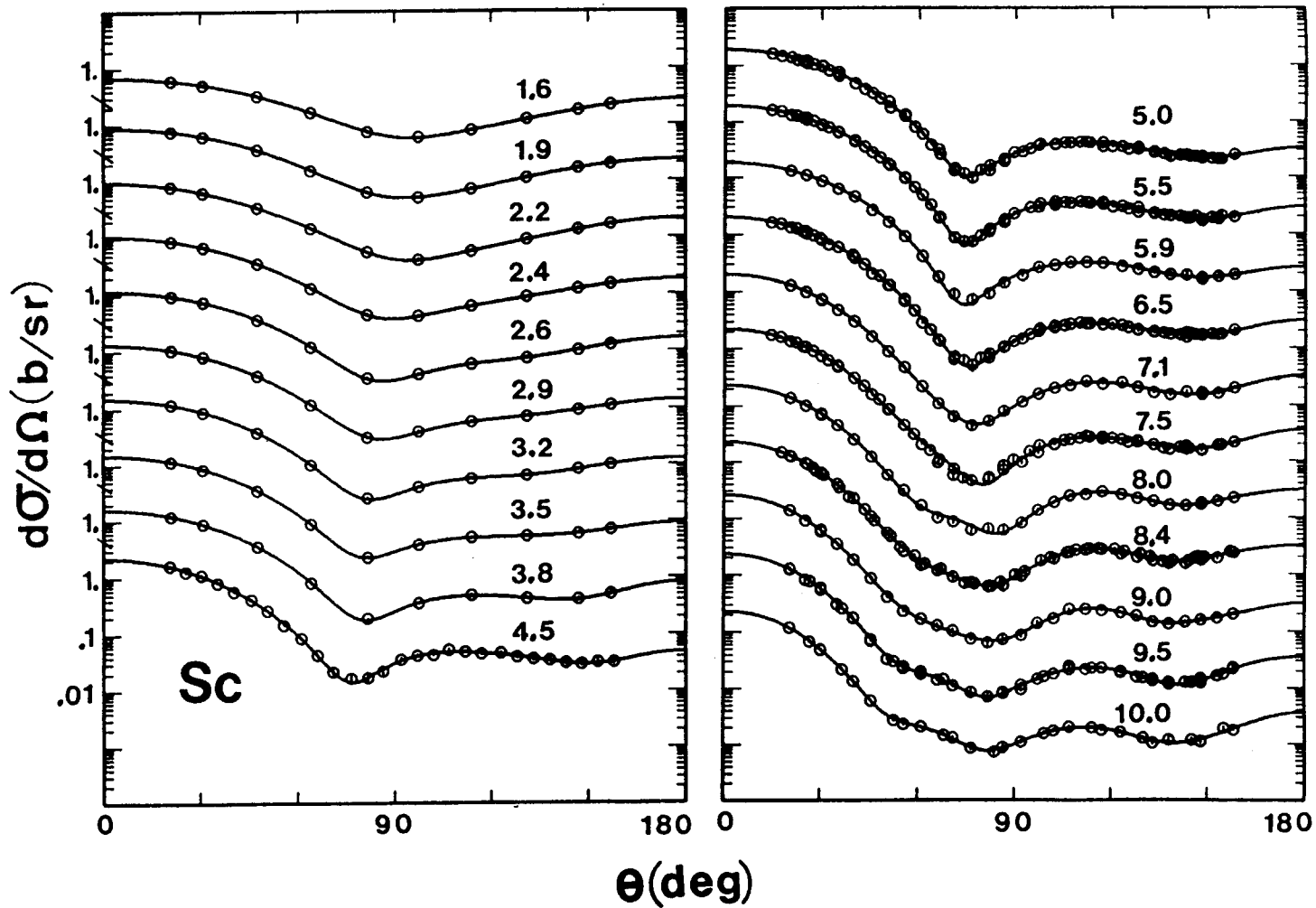


Fig. III-2. Measured differential elastic-scattering cross sections of scandium (symbols). Below 4 MeV the illustrated results are a broad energy averages of the more detailed measurements of Fig. III-1. Approximate incident energies in MeV are numerically given in each portion of the figure. Curves indicate the results of fitting the measured values with Legendre-polynomial expansions.

B. Inelastic Neutron Scattering

There is a dichotomy in the present inelastic-scattering measurements. Relatively broad incident-neutron energy resolutions are employed so as to obtain a good representation of energy-averaged cross-section behavior consistent with the concepts underlying the models used in the interpretations of Section IV. Such broad incident-energy spreads compromise the ability to resolve the inelastically-scattered neutron groups. The dichotomy is unavoidable if the results over a wide energy range are to be obtained in a practical period of time. Another problem inhibiting the inelastic-scattering measurements is the presence of a very low-lying excited level in ^{45}Sc (12.4 keV, $3/2^+$). As noted above, this level could not be experimentally resolved from the elastically-scattered component. It was dealt with in the model interpretations, as described in Section IV, below.

The second and third excited levels in ^{45}Sc are at 377 ($3/2^-$) and 543 ($5/2^+$) keV, respectively. Scattered neutrons due to the excitation of these two levels have energies very close to those resulting from elastic scattering of the second neutron group from the $^7\text{Li}(p,n)^7\text{Be}$ source reaction. As a result, corrections for the second component of the source reaction had to be made. These were an inherent part of the Monte-Carlo correction procedures outlined in Section II, above. The corrections are believed to be reliable, but they did introduce additional uncertainties which particularly compromised knowledge of the angular distributions of the respective scattered neutrons. The observed scattered neutron group corresponding to a mean excitation of 465 keV was attributed to the composite contributions from these two levels. The corresponding scattered-neutron angular distributions did not significantly deviate from symmetry about 90° .

An observed neutron group corresponding to an excitation of 737 keV appears to be clearly associated with the reported level at 720 ($5/2^-$) keV. The next observed excitation is at 1.017 MeV, and is attributed to the composite contributions of reported $0.939(1/2^+)$, $0.974(7/2^+)$ and $1.067(3/2^-)$ levels. Similarly, observed excitations of 1.251, 1.432 and 1.692 MeV were attributed to the reported levels at $\{1.237(11/2^-), 1.303(3/2^+)\}$, $\{1.409(5/2^-, 7/2^-), 1.433(9/2^+), 1.556(3/2^-)\}$ and $\{1.662(9/2^-), 1.800(5/2^+)\}$ MeV, respectively. All of the angular distributions of the scattered neutrons did not significantly differ from symmetry about 90° . These correlations of observed and reported level structures are defined in Table III-1, and

schematically illustrated in Fig. III-3.

Angle integrated cross sections corresponding to the above observed excitations were determined by fitting the observed differential cross sections with low-order (usually 2 or 3) Legendre-polynomial expansions. The angle integrated results were then averaged over ≈ 100 keV to further smooth fluctuations. The results are illustrated in Fig. III-4. The illustrated uncertainties are subjective estimates, including considerations of both systematic and statistical uncertainties. The results extend up to incident energies of ≈ 4 MeV. At higher incident energies the observed inelastic groups for these discrete levels were very small, suggesting largely compound-nucleus processes. There are no directly-comparable results available in the literature. At lower energies, Barnard et al. [13] have reported inelastic-scattering cross sections for the excitation of the first several levels. Their results show large resonance fluctuations, but, when averaged over ≈ 100 keV, are reasonably consistent with the present work as illustrated in Fig. III-4. In addition, there are several reported $(n;n,\gamma)$ results [15,16]. However, these are difficult to unambiguously relate to neutron cross sections.

IV. PHYSICAL MODELS

The physical modeling of the above experimental results had three objectives. First, an assessment of the suitability of a conventional optical-statistical model a few nucleons away from the doubly-closed shell at ^{40}Ca , in the region of appreciable compound-nucleus processes, was sought. In this area, the conventional interpretation of the neutron interaction with ^{40}Ca has proven difficult [1,2]. Secondly, the effect of the dispersion relationship [17] on the optical-model interpretation was examined. And thirdly, a simple model for quantitative extrapolation of the measured values for applied purposes, as described in the companion document outlining the use of the model for the provision of a comprehensive evaluated neutronic data file for elemental scandium [3].

A. Optical-Statistical Model (SOM)

This portion of the interpretation follows methods extensively employed at this laboratory for a number of years, therefore only an outline is given here [18-20]. Conventional Woods-Saxon real, Woods-Saxon derivative imaginary, and Thomas spin-orbit potential forms were assumed [21]. Compound-nucleus processes were calculated using the Hauser-Feshbach theory [22], as modified by Moldauer [23]. Fifteen discrete levels to excitation energies of ≈ 1.8 MeV were taken from ref. [14], as defined in Table III-1. Higher-energy excitations

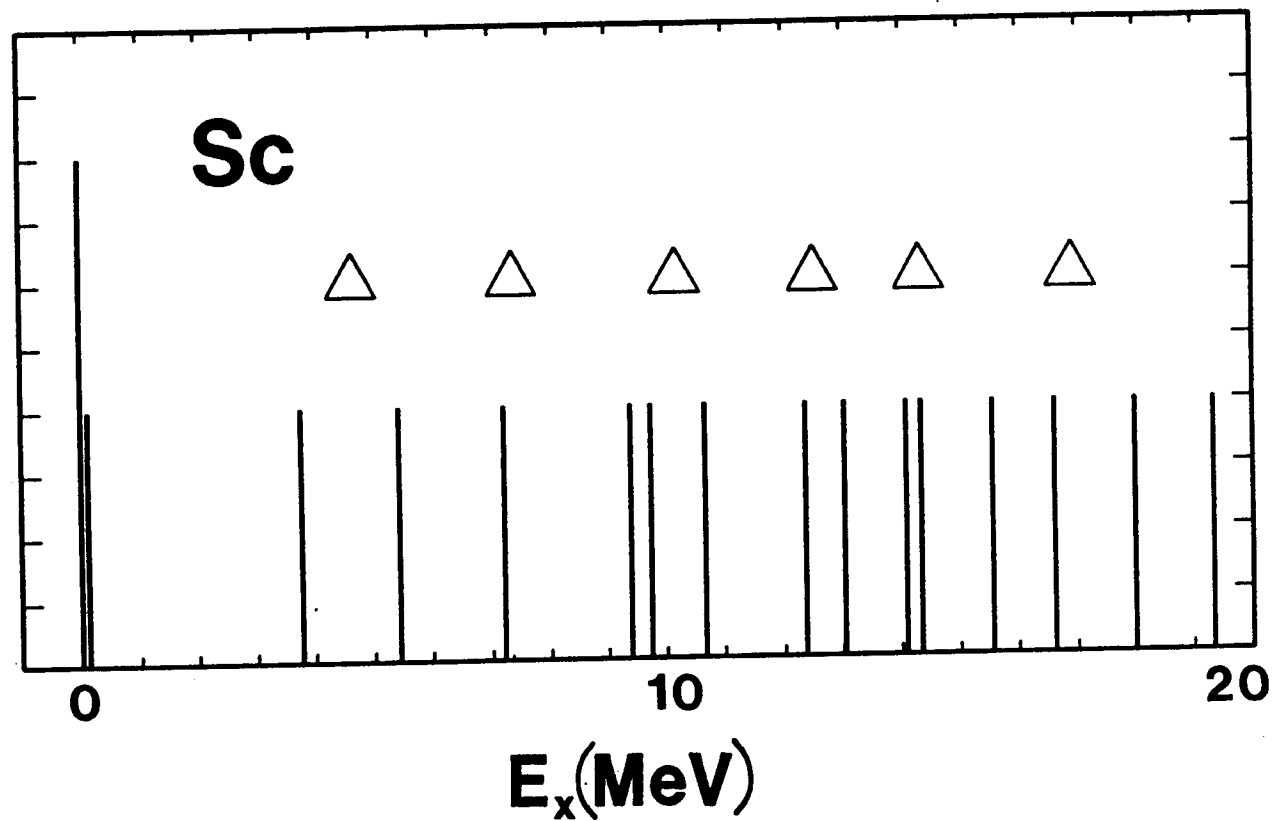


Fig. III-3. Schematic correlation of the ^{45}Sc level excitations as given in the literature (vertical bars) [14] with those observed in the present measurements (triangles).

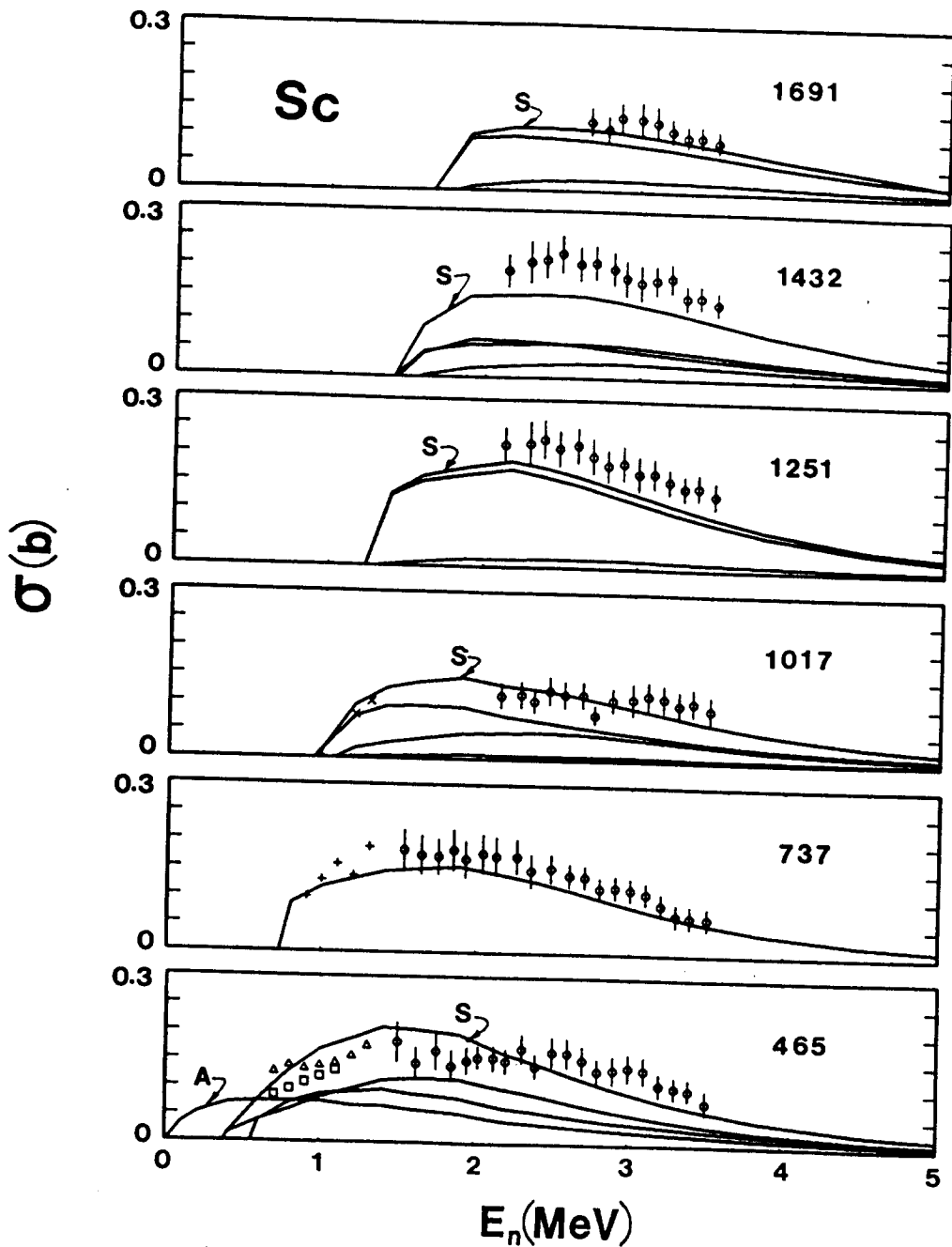


Fig. III-4. Neutron inelastic-scattering excitations of scandium. The present experimental results are represented by "0" symbols, and those of ref. [13] by \square (377 keV level), Δ (543 keV level), $+$ (720 keV level) and \times (939 keV level). Curves are the results of calculations as described in the text. Where more than one level contributes to the observed excitation the calculated sum is indicated by "S". "A" indicates the calculated excitation of the 12.4 keV level. The observed excitation energies are numerically given in the respective portions of the figure.

Table III-1. Comparison of Reported Excited Levels in ^{45}Sc [14] with Excitation Energies Observed in the Present Work (in MeV)

| No. | Level ^a | E_x (observed) |
|-----|---|--------------------------|
| 1 | 0.000(7/2 ⁻) | 0.0 ^b |
| 2 | 0.012(3/2 ⁺) | |
| 3 | 0.377(3/2 ⁻) | 0.465±0.023 ^c |
| 4 | 0.543(5/2 ⁺) | |
| 5 | 0.720(5/2 ⁻) | 0.737±0.020 ^c |
| 6 | 0.939(1/2 ⁺) | 1.017±0.034 ^c |
| 7 | 0.974(7/2 ⁺) | |
| 8 | 1.068(3/2 ⁻) | |
| 9 | 1.237(11/2 ⁻) | 1.251±0.020 ^c |
| 10 | 1.303(3/2 ⁺) | |
| 11 | 1.409(5/2 ⁻ , 7/2 ⁻) | 1.432±0.023 ^c |
| 12 | 1.433(9/2 ⁺) | |
| 13 | 1.556(3/2 ⁻) | |
| 14 | 1.662(9/2 ⁻) | 1.691±0.025 ^c |
| 15 | 1.800(5/2 ⁺) | |

^a Taken from ref. [14].

^b Not experimentally resolved, see text.

^c Uncertainties are the RMS deviation of a number of measured values from the average, not to be confused with scattered-neutron resolutions.

were estimated using the statistical formulation of Gilbert and Cameron [24]. All of the calculations were carried out using the computer code ABAREX [25]. That code has the capability to calculate and fit data consisting of composites of levels. In this particular application, the calculated elastic scattering and the inelastic scattering due to the excitation of the very low-lying first-excited level (12.4 keV) were combined so as to be consistent with the experimental measurements outlined above. This inelastic contribution to the elastic scattering is very small (< 5 mb/sr) over the energies of the present interpretation, as illustrated by the calculated results of Fig. III-4 (curve "A"). There is apparently no polarization information for scandium in the literature, therefore the global spin-orbit potential of Walter and Guss [26] was assumed throughout the calculations, averaged to the mean energy of the present interpretation.

The potential parameters of the model were determined by explicitly chi-square fitting the measured elastic-scattering angular distributions. These consisted of the present measurements (outlined in Section III), augmented with 200 keV averages of the lower-energy results of Barnard et al. [13]. In order to smooth any persistent fluctuations, and in order to reduce the magnitude of the calculational endeavor, the present elastic-scattering results below 4 MeV were further averaged over ≈ 300 keV incident-energy increments, with the results illustrated in Fig. III-2. This elastic-scattering data base extends from a few-hundred keV to 10 MeV. There is no higher-energy elastic scattering information. Subjective consideration was given to the total cross section to 20 MeV, to the prominent inelastic excitation processes, and to the strength functions deduced from resonance measurements [27]. The fitting started by determining the geometric parameters of the real potential as experience has shown them to be more of a "regional" or even "global" nature, not greatly influenced by the particular nuclear structure involved [18-20]. First the real diffuseness, a_v , was determined, and then the reduced real radius, r_v (herein all radii are expressed in the form $R_i = r_i \cdot A^{1/3}$). With the real-potential geometries fixed, the fitting then addressed the imaginary potential geometries, first dealing with the radius, r_w , and then the diffuseness, a_w . Finally, two parameter fitting was used to determine the real- and imaginary-potential strengths. Since some of the model geometries are energy dependent, the potential strengths are given in terms of volume-integrals-per-nucleon, J_i .

The resulting SOM parameterization (see Table IV-1) gives a very acceptable description of the differential elastic-scattering data base from which it was developed, as shown in Fig. IV-1. The real- and imaginary-potential strengths have reasonable values and energy dependencies, as shown in Fig. IV-2. The real strength decreases with

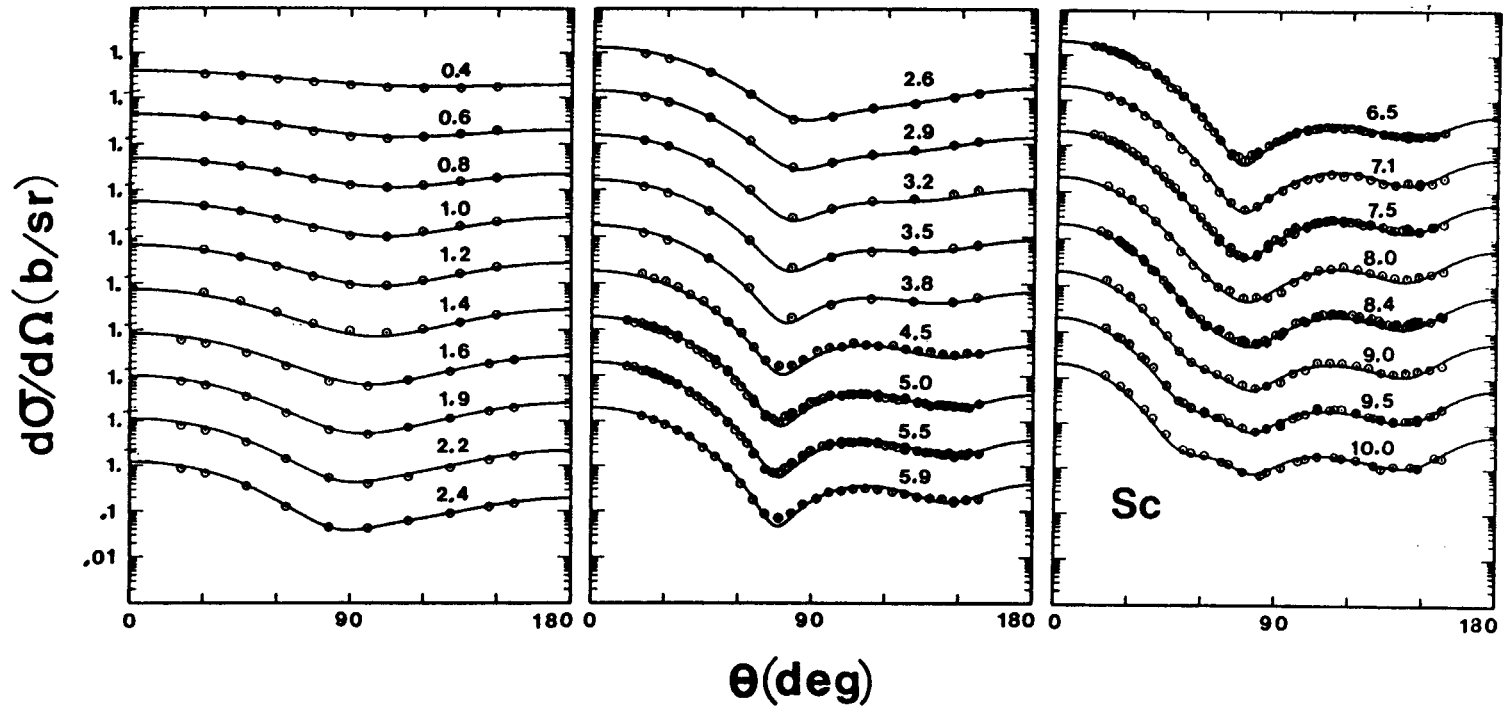


Fig. IV-1. Comparison of measured differential elastic-scattering cross sections (symbols) with the prediction of the SOW (curves). The data is defined in the text. Approximate incident-neutron energies in MeV are noted on the figure.

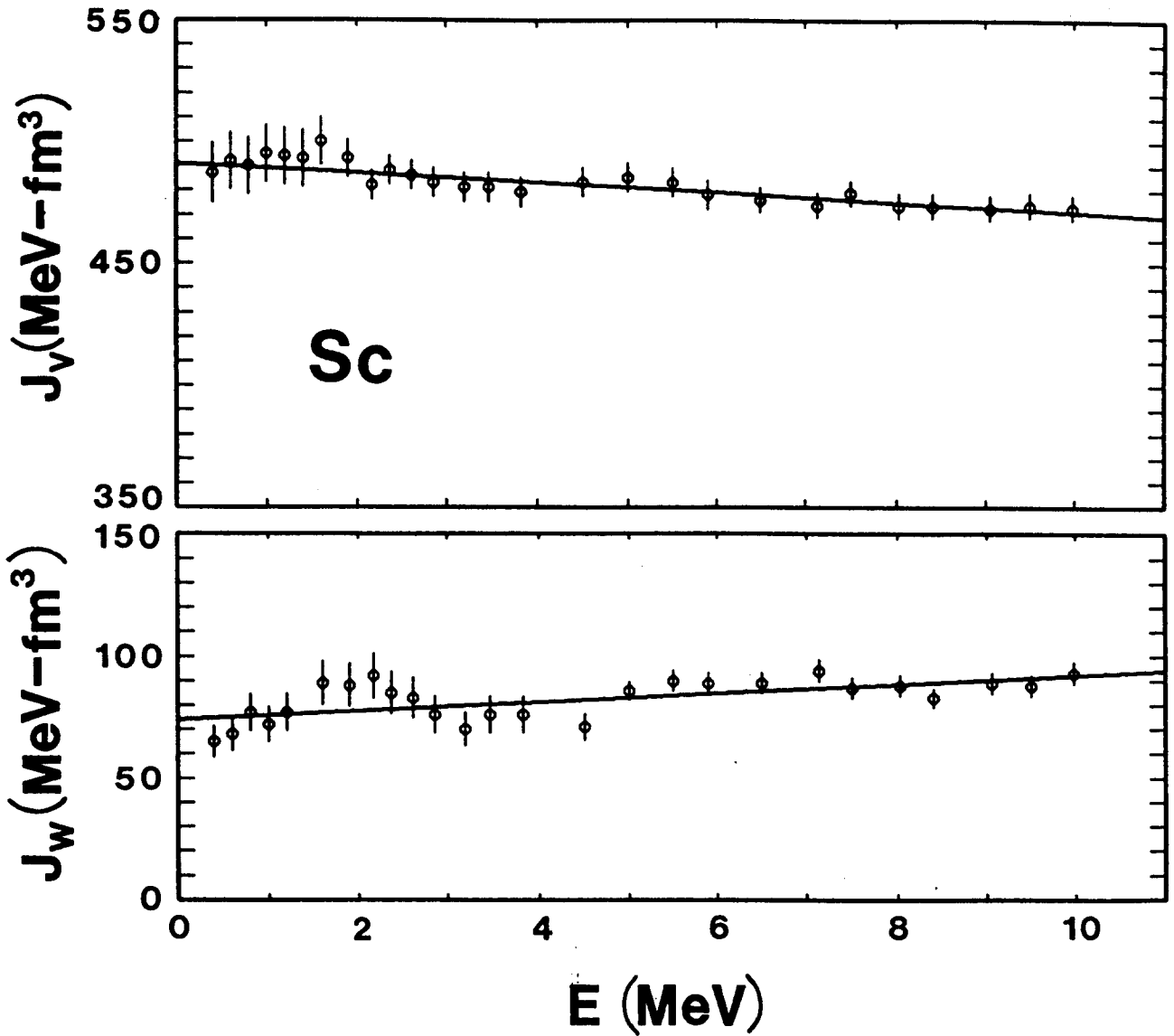


Fig. IV-2. Real (J_v) and imaginary (J_w) SOM potential strengths in terms of volume-integrals-per-nucleon. Values derived from the fitting procedures are noted by symbols while curves represent the parameterization of Table IV-1.

Table IV-1. SOM parameters obtained from the fitting procedures. Geometric quantities are given in fermis, and strengths as volume-integrals-per-nucleon (in MeV-fm³), excepting the spin-orbit potential which is in MeV. The parameters are based upon analysis to 10 MeV as described in the text.^a

Real Potential

$$\begin{aligned}J_v &= 490.96 - 1.9627 \cdot E \\r_v &= 1.2644 \\a_v &= 0.5918 + 0.01355 \cdot E\end{aligned}$$

Imaginary Potential

$$\begin{aligned}J_w &= 74.07 + 1.8089 \cdot E \\r_w &= 1.4799 - 0.02202 \cdot E \\a_w &= 0.2243 + 0.20898 \cdot E - 0.001379 \cdot E^2\end{aligned}$$

Spin-orbit Potential

$$\begin{aligned}V_{so} &= 5.382 \\r_{so} &= 1.020 \\a_{so} &= 0.500\end{aligned}$$

^a Numerical values are given to enough significant figures to permit accurate reproduction of the calculations, and do not necessarily imply the accuracies of the parameters.

energy as one would expect from a Hartree-Fock behavior, and the imaginary strength increases with energy due to the increasing number of channels not explicitly dealt with in the calculations. The neutron total cross section is compared with experimental measurements in Fig. IV-3. The calculated shape and magnitudes are very close to those of the measurements of ref. [28], but not with those of ref. [29]. The calculated minimum of the cross section at ≈ 1 MeV is somewhat larger than suggested by the measurements of ref. [13], but the difference is not large, and it is a region of large cross-section fluctuations. The SOM gives a reasonable description of inelastic scattering where the processes are primarily due to compound-nucleus processes, as shown in Fig. III-4. This result, and the comparisons of Fig. IV-1, indicate that the SOM reasonably predicts the compound-nucleus absorption cross section. The calculated s-wave strength function is 3.01×10^{-4} , to be compared with $4.7 (\pm 0.8) \times 10^{-4}$ deduced from resonance measurements [27]. Strength functions in this region fluctuate by large amounts, so the SOM prediction is acceptable.

The physical implications of this SOM are discussed in Section V, below.

B. Dispersive Optical Model (DOM)

The dispersion relationship correlates real and imaginary portions of the optical potential [17]. Expressed in terms of volume-integrals-per-nucleon, it takes the form

$$J_v(E) = J_{HF}(E) + \frac{P}{\pi} \int_{-\infty}^{+\infty} \frac{J_w(E') dE'}{(E-E')}, \quad (IV-1)$$

where P is the principal value of the integral and J_{HF} the Hartree-Fock component. The integral can be broken into surface, $\Delta J_s(E)$, and volume, $\Delta J_{v0}(E)$, components, and thus

$$J_v(E) = J_{eff}(E) + \Delta J_s(E), \quad (IV-2)$$

where $J_{eff}(E) = J_{HF}(E) + \Delta J_{v0}(E)$. The SOM interpretation, above, gives no support to the presence of a volume absorption to at least 10 MeV, and, since both J_{HF} and ΔJ_{v0} are approximately linear functions of the energy to at least 20 MeV [19], they are not experimentally separable. For computational purposes, the ratio

$$\lambda(E) = \Delta J_s(E)/J_s(E) \quad (IV-3)$$

is defined, where $\lambda(E)$ is the quantity by which the surface imaginary

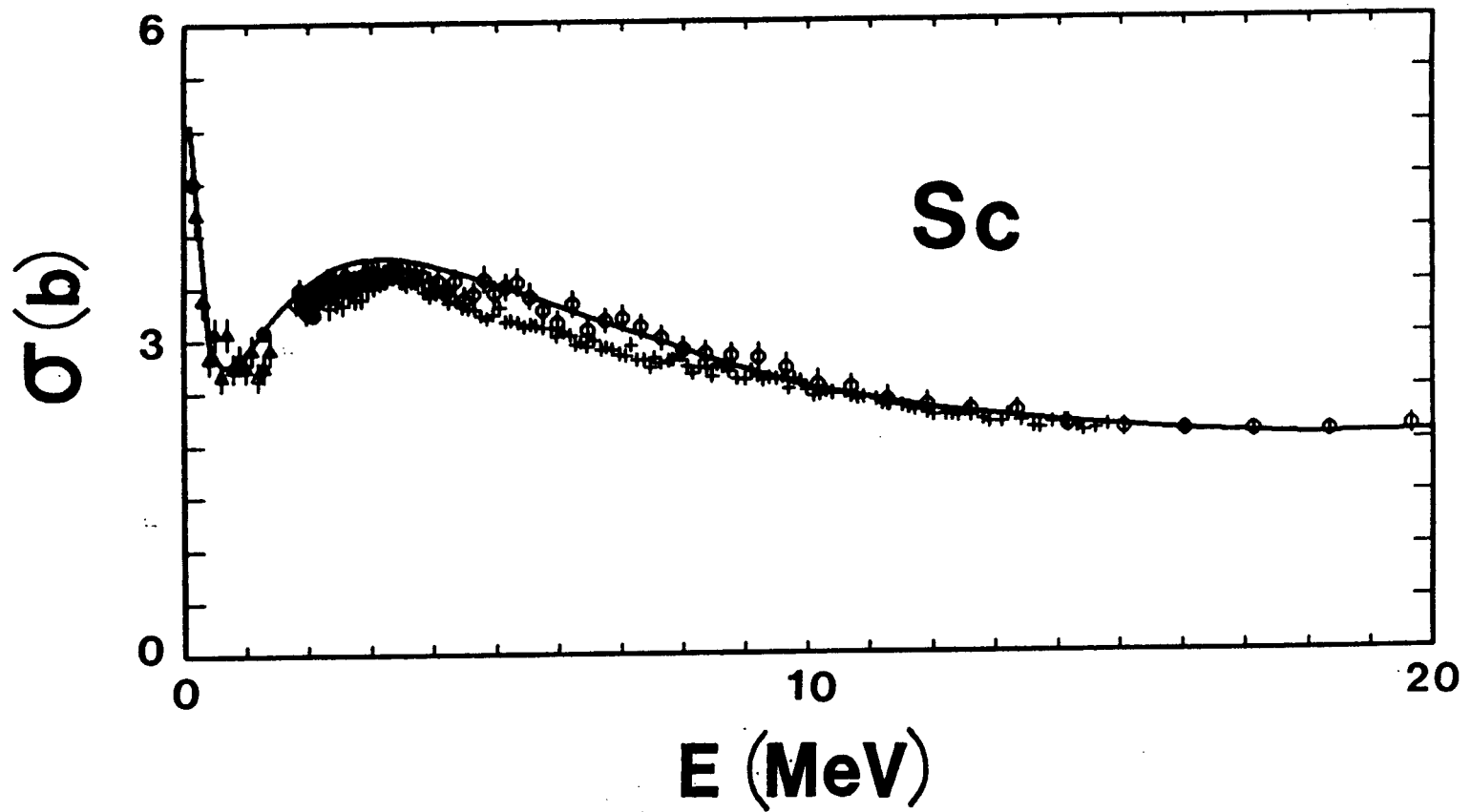


Fig. IV-3. Measured (symbols) and SOM calculated (curve) neutron total cross sections of scandium. The measured values are from refs. 0 = 28, + = 29, and Δ = 13.

potential is multiplied to give the surface peaked term of the real potential, ΔJ_s . The integral of Eq. IV-1 can be readily evaluated using simple approximations frequently employed at this laboratory [e.g., 18-20]. J_s was assumed to be symmetric about the Fermi Energy, E_F . E_F was taken to have the value -10.04 MeV, as deduced from the energies of particle and hole states [30]. For $2E_F < E < 0$, J_s was assumed to have the parabolic form $J_s = (J_0/E_F^2)(E-E_F)^2$ with J_0 equal to $J_s(E=0)$. For $0 < E < 15$ MeV, J_s was taken to have the form of Table IV-1. Above 15 MeV J_s was assumed to decrease linearly with energy to a zero value at 60 MeV. The 15 MeV break point and the 60 MeV cutoff point are reasonable, but there is no experimental evidence to support them. With these assumptions, ΔJ_s and $\lambda(E)$ were calculated, using the SOM potential, above, as a starting point, with the results shown in Fig. IV-4, -5. The net effect of the integral of Eq. IV-1 is to add a significant surface term to the Woods-Saxon Hartree-Fock potential at low energies and to subtract a somewhat smaller component at the higher energies.

The entire fitting procedure used for the SOM was repeated including the surface component of the real potential given by $\lambda(E)$ of Eq. IV-3. The resulting model parameters are given in Table IV-2. Fig. IV-6 shows the real- and imaginary-potential strengths obtained for the DOM. As expected, they differ somewhat from those of the SOM (see Fig. IV-2) as one is dealing with $J_{\text{eff}}(E)$ of Eq. IV-2, rather than the entire volume integral J_v . The physical interpretation of these parameters, and their correlation with those of the SOM, are discussed in Section V. The DOM provides a description of the elastic scattering very similar to that obtained with the SOM, as illustrated in Fig. IV-7. Likewise, the description of the measured total cross sections, and the inelastic-scattering cross sections are essentially equivalent to those obtained with the SOM, and illustrated in Figs. IV-3 and III-4. The calculated $l = 0$ strength function is 3.52×10^{-4} , again, similar to that obtained with the SOM and in acceptable agreement with the value deduced from resonance measurements.

V. DISCUSSION

The above SOM is reasonably "conventional". J_v decreases with energy as the major contribution is from the Hartree-Fock potential, albeit with a slope that is somewhat less than usually observed [18-20]. r_v is similar to that found in this lighter-nuclei region [19]. a_v slightly increases with energy. The slope is small, perhaps

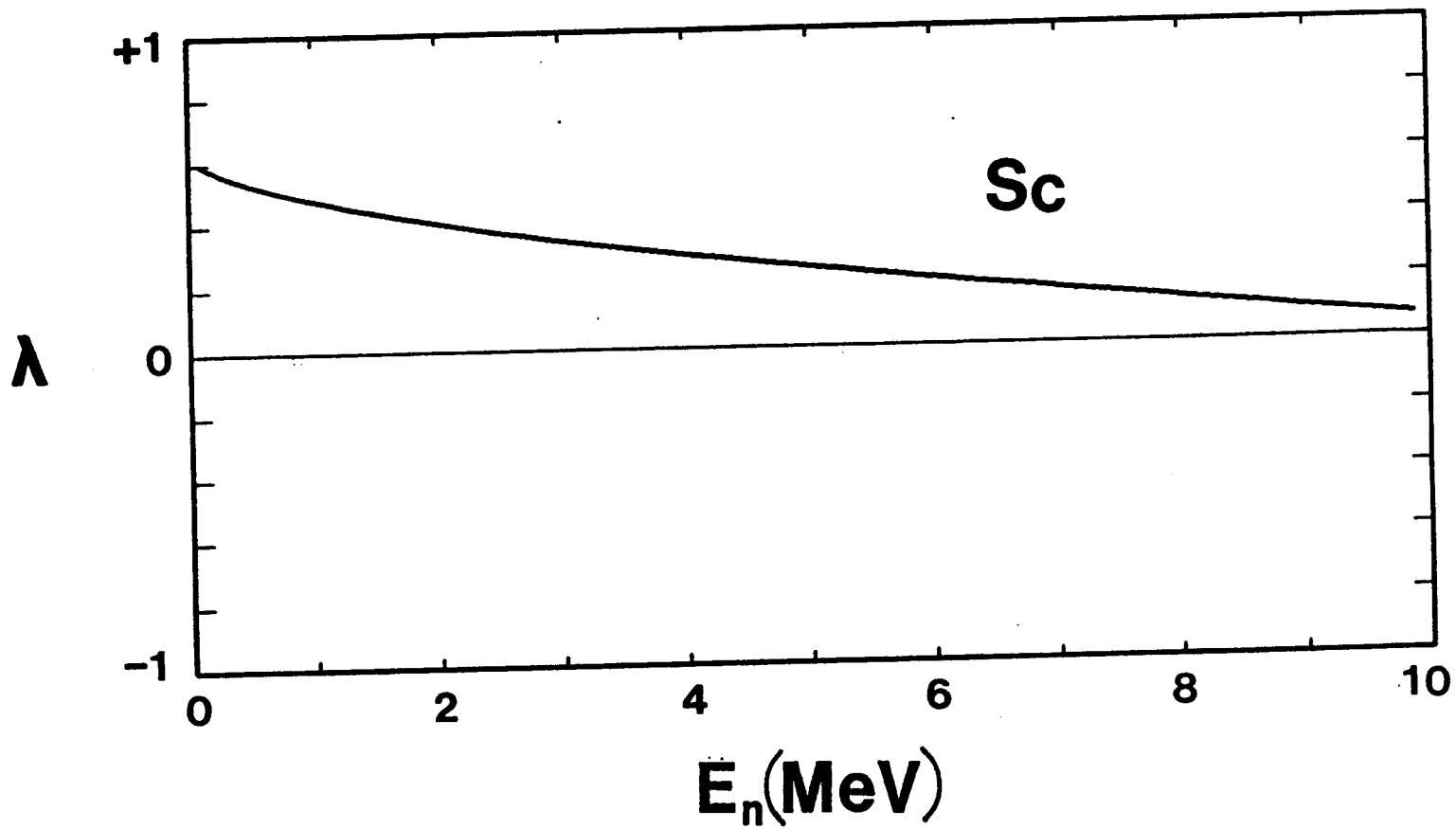


Fig. IV-4. The magnitude and energy dependence of $\lambda(E)$ of Eq. IV-3.

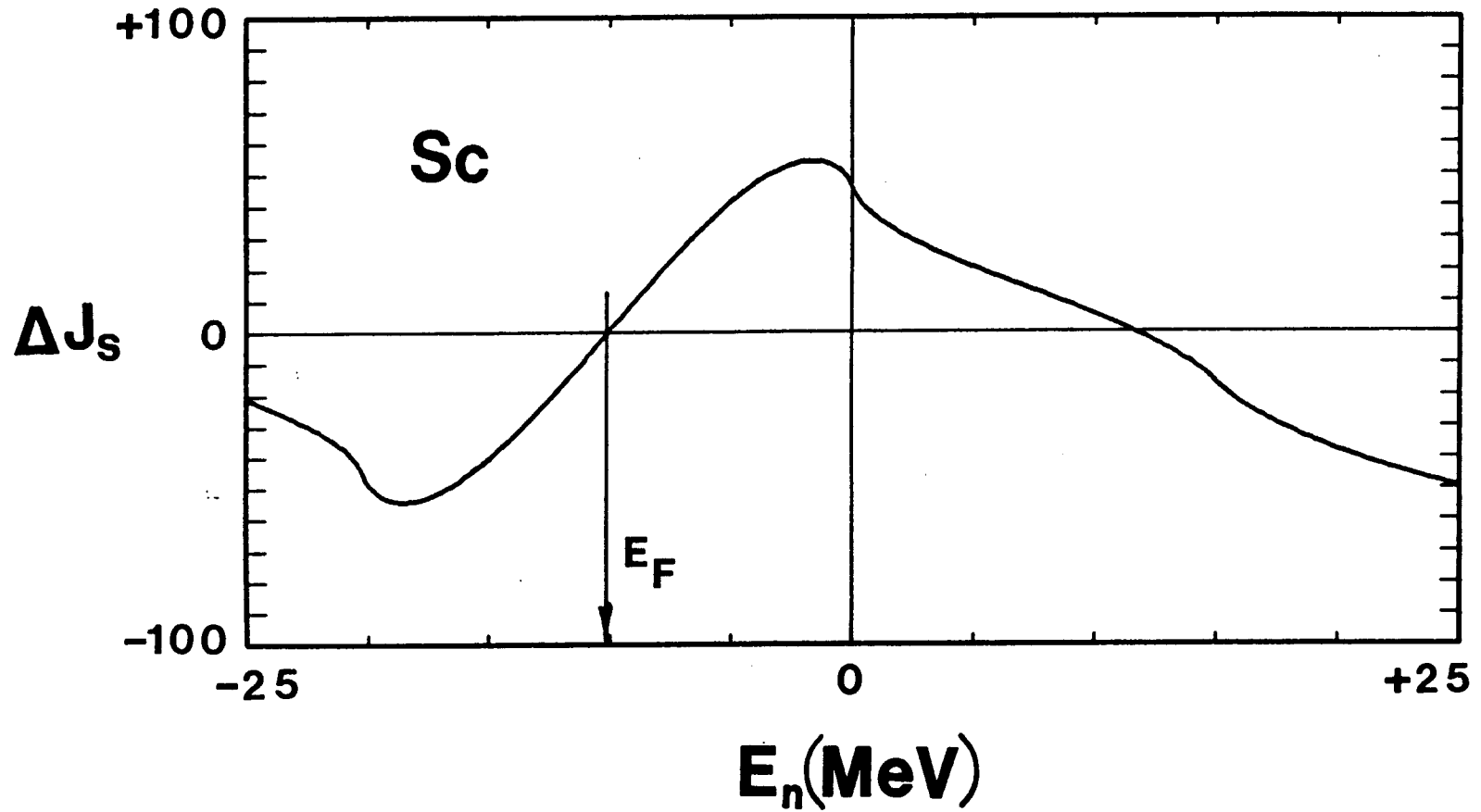


Fig. IV-5. $\Delta J_s(E)$ implied by Eq. IV-1, calculated as described in the text.

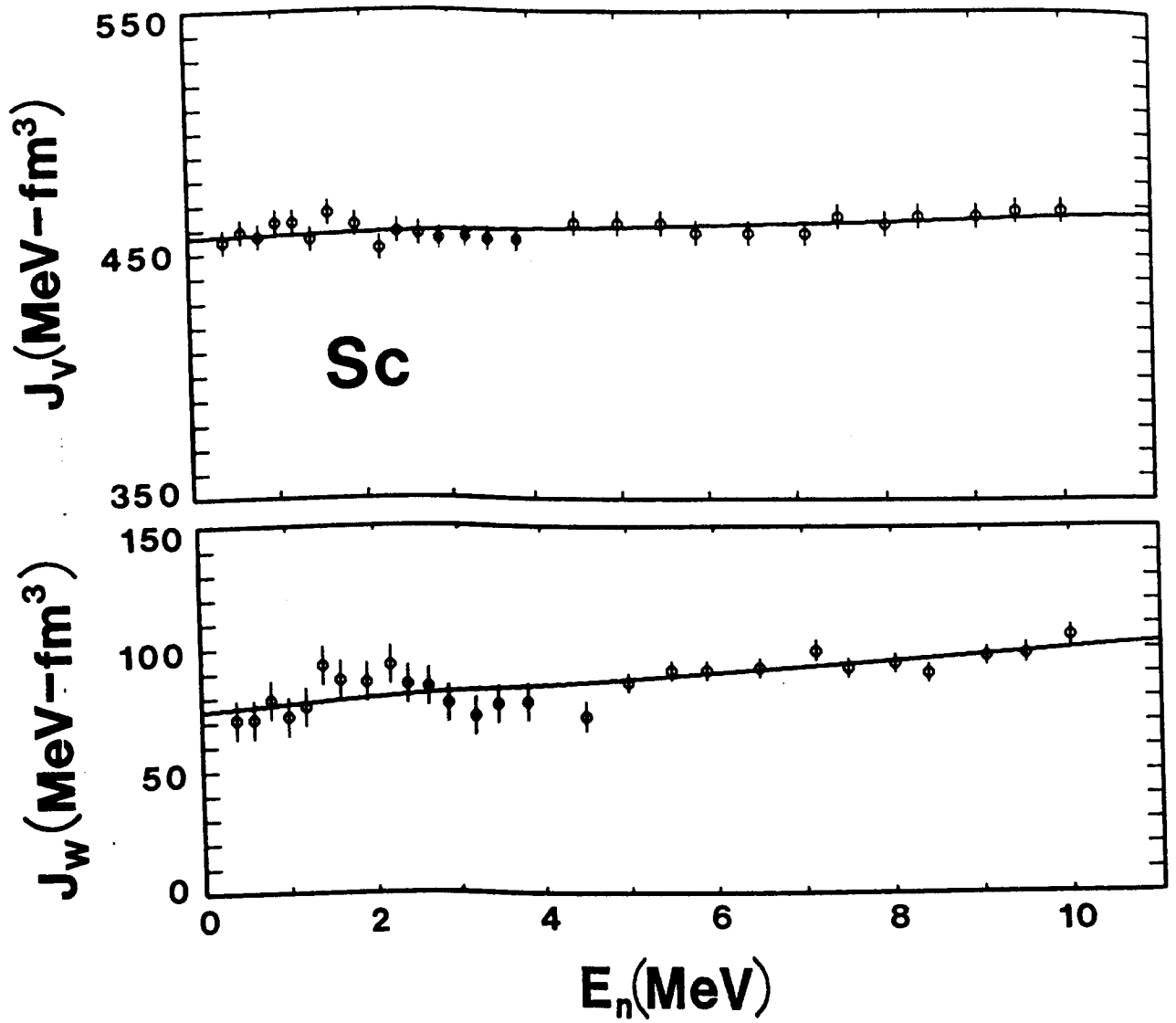


Fig. IV-6. Real, J_v , and imaginary, J_w , DOM potential strengths. Data symbols indicate the results of the fitting procedure and curves the general trends as given in Table IV-2.

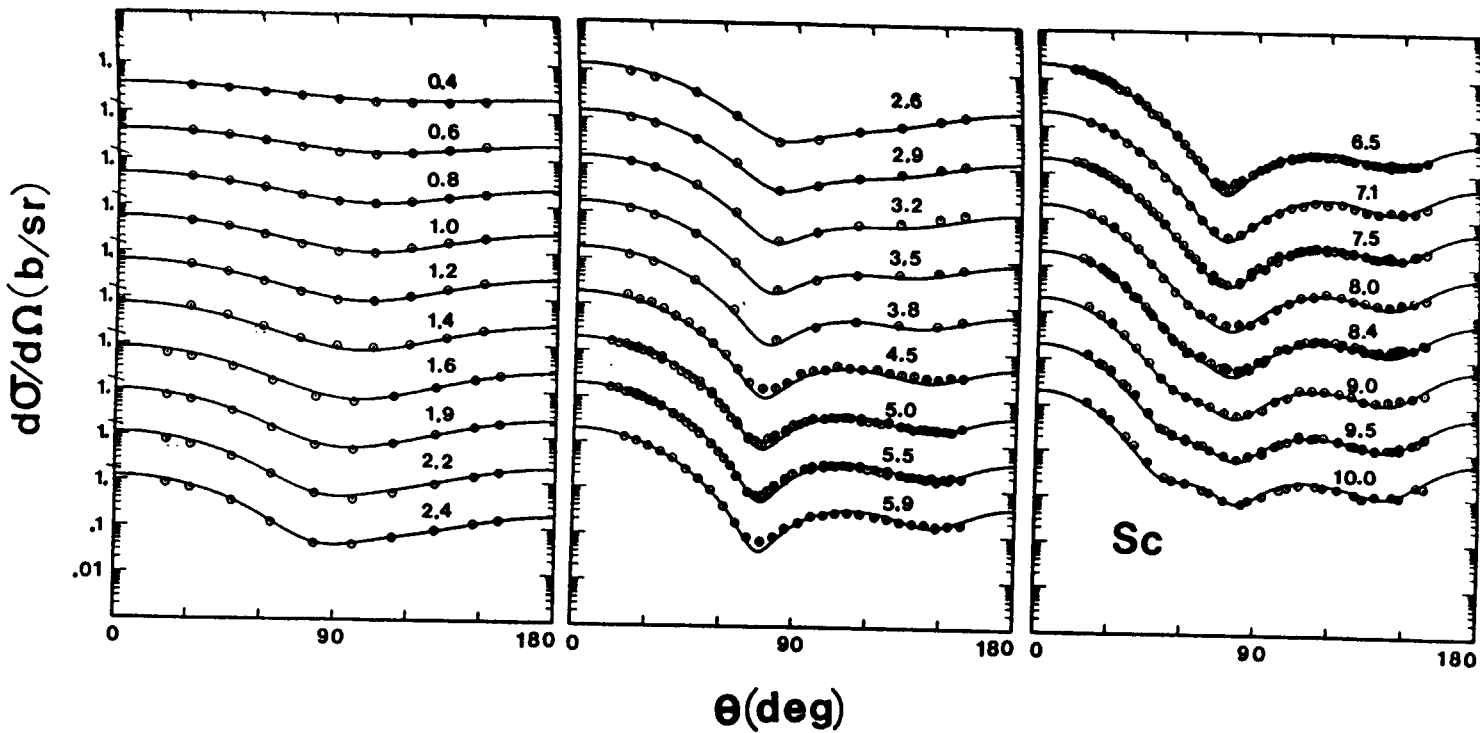


Fig. IV-7. Comparison of measured (symbols) elastic-scattering cross sections with those calculated with the DOM. The notation is identical to that of Fig. IV-1.

Table IV-2. DOM parameters obtained from the fitting procedures. Geometric quantities are given in fermis, and strengths as volume-integrals-per nucleon (in MeV-fm³).

Real Potential

$$J_{\text{eff}} = 456.93 + 0.8749 \cdot E$$

$$r_{\text{eff}} = 1.2330$$

$$a_{\text{eff}} = 0.60273 + 0.017211 \cdot E$$

Imaginary Potential

$$J_w = 74.646 + 2.5363 \cdot E$$

$$r_w = 1.4142 - 0.01128 \cdot E$$

$$a_w = 0.23652 + 0.025685 \cdot E - 0.0015324 \cdot E^2$$

Spin-orbit Potential (same as given in Table IV-1)

only marginally significant, and the average value is ≈ 0.65 fm which is consistent with values commonly encountered in neutron SOM interpretations. The imaginary potential strength, J_w , increases with energy as one would expect from the opening of additional channels. The magnitude is somewhat larger than observed for even targets near shell closures [18], possibly due to the increased level density of the odd scandium target. r_w slowly decreases with energy and is larger than r_v throughout the measured range. As $E \rightarrow 0$, r_w becomes considerably larger than r_v , as was noted from strength-function considerations long ago [31]. a_w becomes quite small as $E \rightarrow 0$. This behavior has also been frequently observed [18-20], and contributes to the good representation of the neutron total cross section at ≈ 1 MeV, as shown in Fig. IV-3. "Global" potentials tend to significantly over-predict the neutron total cross section in this region. The various geometric energy dependencies are, of course, valid only for $E \leq 10$ MeV. There is no experimental information to test their behavior at higher energies, but it is reasonable to expect the geometric parameters to asymptotically approach energy-independent values as the energy increases above ≈ 10 MeV.

The simple SOM reasonably describes the observed neutron interactions with scandium (see Section IV), and thus provides a useful tool for interpolating and extrapolating measured data for applied purposes. Just such an application is described in the companion report [3] documenting a comprehensive evaluated neutronic data file for scandium. The provision of such a quantitative model for applications use was an objective of this work.

It should be clearly noted that the present SOM, employing conventional compound-nucleus formalism with well established width-fluctuation and correlation corrections [23], very nicely describes the compound-nucleus contributions to both elastic and inelastic scattering processes. Even in the most acute minima of the elastic distributions, the calculated and measured cross sections agree to better than several mb/sr (see Fig. IV-1). At the same time the inelastic neutron scattering is, at least qualitatively, described as illustrated in Fig. III-4. Thus the common SOM, with the conventional compound-nucleus formalism including width function and correlation corrections, is a suitable model for the neutron interaction with scandium. In particular, the absorption cross section is reasonably predicted by the model. This result is in contrast with the situation that is frequently encountered when dealing with similar processes in the neighboring doubly-magic target ^{40}Ca [1,2,32]. This dichotomy is further examined in ref. [2].

The DOM leads to results that are generally consistent with those of the SOM. As expected, J_v is reduced as it is really the J_{eff} of

Eq. IV-2, and thus lacks the ΔJ_s contribution. The real radius of the DOM is somewhat smaller than that of the SOM, as the surface component of the real potential, given by $\lambda(E)$ of Eq. IV-3, has been removed. The DOM real potential should be largely devoid of structure effects and thus more nearly approach a "global" parameter. J_{eff} of the DOM is essentially constant with energy. This suggests that the ΔJ_{v_0} of Eq. IV-2 is rather sharply increasing with energy, and/or that the Hartree-Fock potential is essentially energy independent up to ≈ 10 MeV. Either eventuality is uncommon, but perhaps the effect would vanish if there were a wider energy range of experimental information available for the interpretation. The imaginary potential of the DOM is very similar to that of the SOM, with small differences that are probably not significant.

In ref. [20] there is a comparison of the systematic behavior of SOMs at an energy of 8 MeV. At this energy the dispersion effect is generally small (and that is true in the present case of scandium), thus the comparisons should not be particularly sensitive to the dispersion integral of Eq. IV-1. It is suggested in ref. [20] that the real radius of the SOM has a mass dependence of the form

$$r_v = r_0 + r_1/A^{1/3}. \quad (V-1)$$

The present scandium results are consistent with this concept. Indeed, when the r_v results of ref. [20] are extended to include the present scandium results, as shown in Fig. V-1, one obtains the values $r_0 = 1.154$ and $r_1 = 0.4074$ fermis. These are very similar to the results of ref. [20], and are qualitatively consistent with the results reported long ago by Moldauer [31]. With the radial form of Eq. V-1, it was shown in ref. [20] that the systematic behavior of the real SOM strength can be described by

$$J_v = K_0 \cdot [1 - \xi(N-Z)/A] \cdot (r_0 + r_1/A^{1/3})^3, \quad (V-2)$$

where $K_0 = 234.2 \text{ MeV} \cdot \text{fm}^3$ and $\xi = 0.53$. This parameterization was based upon the potentials of refs. [18-20,33-37]. The present scandium SOM potential agrees very well with this parameterization, and when the scandium real potential is added to the data base $K_0 \rightarrow 236.1$ and $\xi \rightarrow 0.575$. These are very modest changes from the values of ref. [20], and the ξ value remains reasonably consistent with that deduced from nucleon-nucleon scattering data ($\xi = 0.48$) [38] and (p,n) results ($\xi = 0.4$) [39], and a factor of approximately two smaller than obtained using the simple isovector expression $J_v = J_0 \cdot [1 - \xi(N-Z)/A]$. Eqs. V-1 and -2, together with $a_v \approx 0.65 \text{ fm}$, form a reasonable starting point for considerations of a "global" real SOM potential. The reliability would increase if the concepts were extended to the DOM

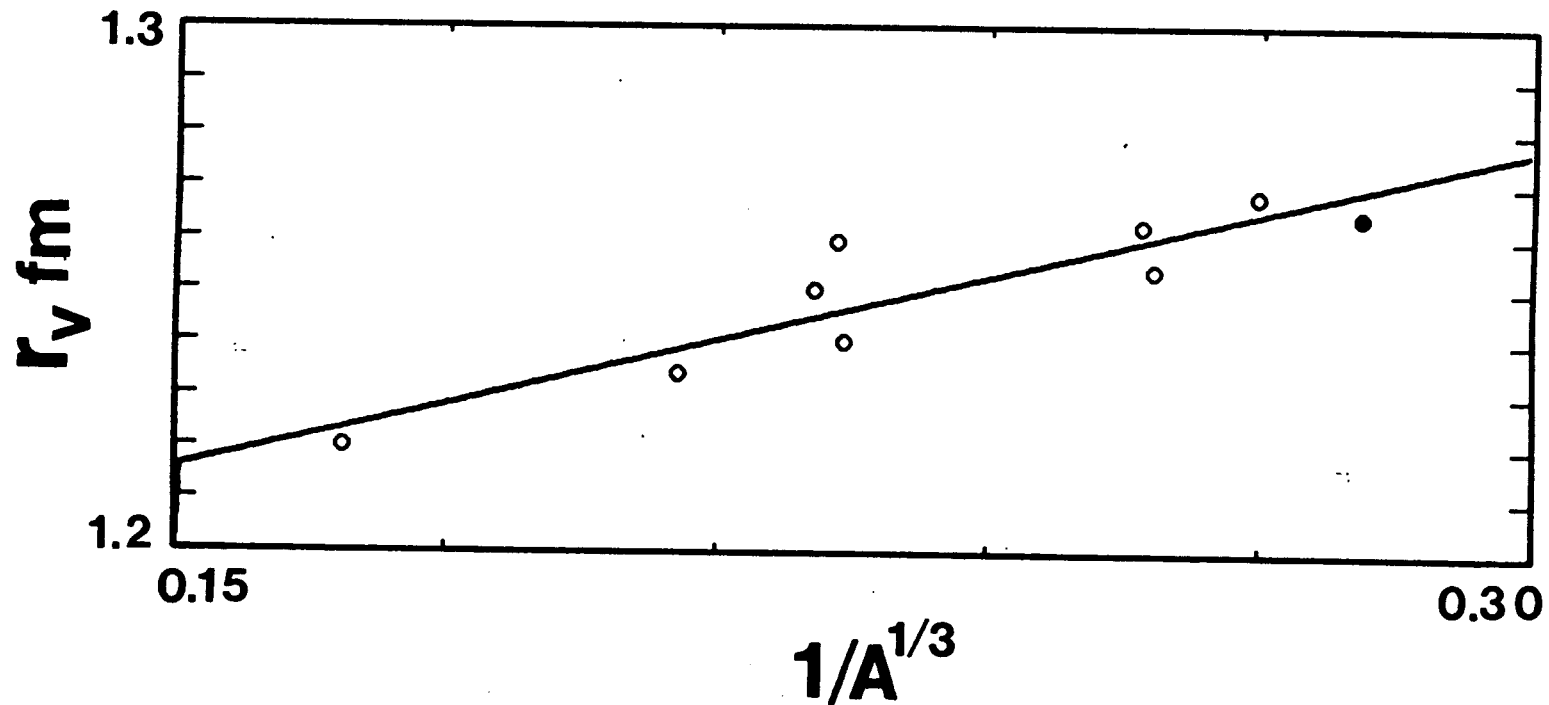


Fig. V-1. Mass, A , dependence of the SOM real-potential radius, r_v . Symbols indicate values taken from interpretations as referenced in the text (the solid point indicates the present scandium value). The curve represents Eq. V-1 fitted to the experimentally-deduced values.

which decouples the structure portion of the real potential from the more general Hartree-Fock form.

Acknowledgement

The authors are indebted to Dr. R. D. Lawson for guidance and suggestion.

References

1. C. H. Johnson and C. Mahaux, Phys. Rev. C38 2589 (1988).
2. A. Smith, P. Guenther, R. Lawson and S. Chiba, ^{40}Ca , the neutron mean field and the compound nucleus, to be published.
3. A. B. Smith, P. T. Guenther and J. W. Meadows, Argonne National Laboratory Report ANL/NDM-126, in press.
4. L. Cranberg and J. Levin, Proc. of Inter. Conf. on Peaceful Uses of Atomic Energy, Geneva, IAEA press (1955); see also, A. Smith, P. Guenther, R. Larsen, C. Nelson, P. Walker and J. Whalen, Nucl. Instr. Methods 50 277 (1967).
5. C. Budtz-Jorgensen, P. Guenther, A. Smith and J. Whalen, Z. Phys. A306 265 (1982).
6. A. Smith, P. Guenther, J. Whalen, W. McMurray, M. Renan and I. van Meerden, Z. Phys. A319 47 (1984).
7. A. Smith, P. Guenther, J. Whalen and S. Chiba, J. Phys. G18 629 (1992).
8. M. Drogg, IAEA TECDOC-410, p. 239, IAEA Press, Vienna (1987).
9. A. Smith, P. Guenther and R. Sjoblum, Nucl. Instr. and Methods 140 3907 (1977).
10. A. Smith, P. Guenther and R. McKnight, Proc. Conf. on Data for Sci. and Technology, edited by K. H. Boeckhoff, Reidel, Dordrecht Holland (1982) p. 39.
11. 1983 Nuclear Standards File IAEA Tech. Report 227, editors H. Conde, A. Smith and A. Lorenz, IAEA Press, Vienna (1983).
12. A. B. Smith, private communication (1990), internal memorandums available from the author.

13. E. Barnard, J. deVilliers, D. Reitmann and J. Teppel, *Z. Phys.* 245 36 (1971).
14. T. W. Burrows, *Nuclear Data Sheets* 40 149 (1983); also *Nuclear Data Sheets* 65 1 (1992).
15. V. C. Rogers et al., *Nucl. Phys.* 137 85 (1969).
16. D. A. Lind, *Ann. Phys.* 12 485 (1961).
17. G. R. Satchler, *Direct Nuclear Reactions* (Clarendon, Oxford, 1983).
18. S. Chiba, P. Guenther, A. Smith, M. Sugimoto and R. Lawson, *Phys. Rev.* C45 1260 (1992).
19. A. Smith, P. Guenther, J. Whalen and S. Chiba, *J. Phys.* G18 629 (1992).
20. S. Chiba, P. Guenther, R. Lawson and A. Smith, *Phys. Rev.* C42 2487 (1990).
21. P. E. Hodgson, *Nuclear Reactions and Nuclear Structure* (Clarendon, Oxford, 1971).
22. W. Hauser and H. Feshbach, *Phys. Rev.* 87 366 (1952).
23. P. A. Moldauer, *Nucl. Phys.* A344 185 (1980).
24. A. Gilbert and A. Cameron, *Can. J. Phys.* 43 1446 (1965).
25. P. A. Moldauer, private communication (1982).
26. R. L. Walter and P. P. Guss, *Proc. Conf. on Nucl. Data for Basic and Applied Science*, edited by P. Young, R. Brown, G. Auchampaugh, P. Lisowski and L. Stewart (Gordon and Breach, New York, 1986) Vol. 2, p. 1079.
27. S. F. Mughabghab, M. Divadeenam and N. E. Holden, *Neutron Cross Sections* (Academic, New York, 1981).
28. W. Poenitz and J. Whalen, Argonne National Laboratory Report ANL/NDM-80 (1982).
29. D. Foster and D. Glasgow, *Phys. Rev.* C3 576 (1971).
30. R. D. Lawson, private communication (1992).
31. P. A. Moldauer, *Nucl. Phys.* 47 65 (1963).
32. D. M. Hetrick, C. Y. Fu, and D. C. Larson, Oak Ridge National Laboratory Report ORNL/TM-8290 (1982).

33. R. D. Lawson, P. T. Guenther and A. B. Smith, Nucl. Phys. A493 267 (1989).
34. R. D. Lawson, P. T. Guenther and A. B. Smith, Phys. Rev. C34 1599 (1986).
35. A. B. Smith, P. T. Guenther and R. D. Lawson, Nucl. Phys. A483 50 (1988).
36. A. B. Smith, P. T. Guenther and R. D. Lawson, Nucl. Phys. A455 344 (1986).
37. R. D. Lawson, P. T. Guenther and A. B. Smith, Phys. Rev. C36 1298 (1987).
38. G. W. Greenlees, W. Makofske and G. J. Pyle, Phys. Rev. C1 1145 (1970).
39. C. J. Batty, E. Friedman and G. W. Greenlees, Nucl. Phys. A127 368 (1969).